Recent Trends in Low-frequency Noise Reduction Techniques for Integrated Circuits

Christian Enz
ICLAB, EPFL
Neuchâtel, Switzerland
christian.enz@epfl.ch

Assim Boukhayma
CEA-LETI, Grenoble, France
EPFL, Neuchâtel, Switzerland
assim.boukhayma@epfl.ch

***Abstract*—This paper presents the two main circuit techniques, namely autozeroing (AZ) and chopper stabilization (CS), that are used to reduce the $1/f$ noise and offset in amplifiers typically used in sensor electronics interfaces. After recalling their main properties, it looks into recent trends in circuit noise reduction techniques. First, the correlated multiple sampling (CMS) technique is presented as a generalization of AZ and correlated double sampling (CDS). Introduced in CMOS image sensors (CIS), it combines noise averaging and canceling and allows to further reduce the $1/f$ noise, but, like AZ, it is also ultimately limited by the aliasing of the broadband white noise. Another technique combining noise canceling and CS in a transimpedance amplifier (TIA) for bio-sensors is presented. It allows to maintain a low input impedance required by the TIA, while reducing the noise of the main transimpedance stage. CS is then used to cancel the noise of the following stages.**

I. Introduction

NOISE represents the ultimate limitation in many sensor signal acquisition electronics systems. Offset is also a serious limitation, but, contrary to noise, it is not as fundamental since it can usually be significantly reduced, whereas noise can be reduced, but it cannot be fully eliminated. For low-frequency applications, the flicker or $1/f$ noise dominates in many integrated CMOS sensor front-ends. Beyond high-pass filtering, which often also filters out the wanted signal, mainly two circuit techniques are used to reduce the dominant $1/f$ noise of MOS transistors: autozero (AZ) and chopper stabilization (CS) techniques. Both approaches allow to significantly reduce the input-referred low-frequency noise and at the same time also the offset. They are particularly well-suited to CMOS integrated circuits since they mostly use switches, made of simple transistors, and capacitors. Initially, both techniques were considered equivalent, but it turned out that they have very different impact on the boadband white noise [1], [2].

Both, AZ and CS techniques have evolved in the recent years, not that much to improve the noise performance further, but mostly to improve the residual offset due spiking. This papers looks at the recent trends in the field of low-frequency noise reduction techniques. The paper is organized as follows: Section II recalls the basic principles of AZ and CS. Section III looks at the recent trends in noise reduction techniques, with a particular emphasis on Correlated Multiple Sampling (CMS) and the combination of noise cancelation and CS.

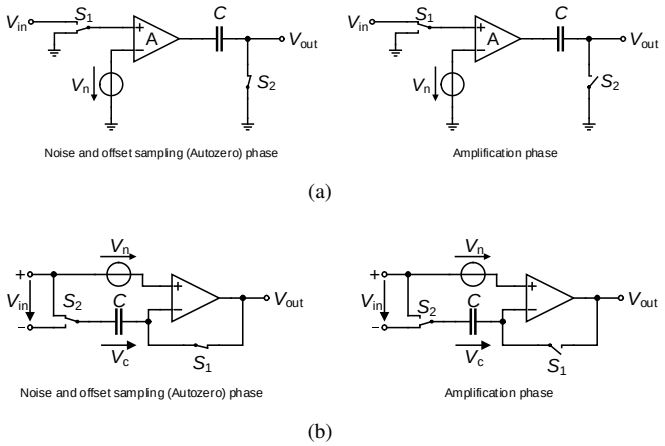

Fig. 1. Example of circuit implementations of the autozero (AZ) principle. a) An open-loop offset-compensation (OLOC) low-gain amplifier [3] and b) a closed-loop offset-compensation amplifier.

II. The Basic Low-frequency Noise and Offset Reduction Techniques

A. The Autozero (AZ) Technique

The basic idea of the autozero (AZ) technique is to sample the unwanted quantity (noise and offset), and then subtracting it from the instantaneous value of the contaminated signal. The AZ process requires at least two phases: a sampling phase (Φ_1) during which the offset and noise voltages are sampled and stored, and an amplification phase (Φ_2) during which the offset-free stage is available for operation. The simplest way to implement AZ is to sample the offset and the noise at the output of the amplifier as initially proposed by Poujois and Borel [4] and illustrated in Fig. 1(a). During the AZ phase corresponding to Fig. 1(a), the input switch S_1 and the output switch S_2 are both connected to ground. Switch S_2 is then opened and the noise and offset voltage V_n multiplied by the amplifier gain A remains stored on capacitor C. This stored output voltage is altered by an error voltage caused by the charge injection occurring at the opening of switch S_2. After the AZ phase, the input terminal of the amplifier is connected back to the signal by switch S_1. The input-referred residual offset is thus limited by the charge injection or charge injection mismatch in the case of a differential implementation. It is

obviously effective only if the amplifier does not saturate during the autozeroing phase. This requires that the output-referred offset remain smaller than the minimum saturation voltage. This is possible only if the amplifier gain is relatively small (typically, less than 10).

The open-loop offset cancellation principle is not well suited to high-gain amplifiers where it is usually preferable to sense the amplifiers offset in a closed-loop configuration as shown in Fig. 1(b) [5]. During the sampling phase, the amplifier is disconnected from the signal path and connected in a unity-gain configuration as shown in Fig. 1(b). Assuming that the open-loop gain A of the amplifier is much larger than 1, the voltage V_c obtained across the storage capacitor C after the amplifier has settled is almost equal to its offset voltage. This voltage (plus an additional error caused by the charge injection occurring when switch S_1 opens) is stored across capacitor C. After this sampling phase, the offset-compensated stage is available for amplification and is connected again to the signal path. The residual offset is nearly equal to the original offset divided by the amplifier dc gain, and is ultimately limited by charge injection. In the schemes described above, the amplifier is not available to the external circuitry during the offset sampling phase. This is not a major drawback for most applications. In case continuous-time amplification is required, the offset-free amplifier can be duplicated and used in a time-shared (ping-pong) operation [6], or the continuous-time feedforward technique may be used [7], [8].

The effect of the AZ process on the amplifier noise can be studied assuming that the input-referred noise of the amplifier corresponding to voltage source V_n in Fig. 1 is written as

$$S_n(f) = S_0 \cdot \left(1 + \frac{f_k}{|f|}\right), \tag{1}$$

where S_0 represents the amplifier input-referred white noise power spectral density (PSD) (usually thermal noise) and f_k is the corner frequency, defined as the frequency for which the $1/f$ noise PSD becomes equal to the white noise S_0. Unlike the offset voltage, which can be considered constant, the amplifiers noise and particularly its wideband thermal noise component is time-varying and random. The efficiency of the AZ process for the low-frequency noise reduction will thus strongly depend on the correlation between the noise sample and the instantaneous noise value from which this sample is subtracted. The autocorrelation between two samples of $1/f$ noise is much higher than for white noise, assuming they have the same bandwidth. The AZ process is thus efficient for reducing the $1/f$ noise but not the broadband white noise. Another way of looking at the effect of autozeroing is to note that it is equivalent to subtracting from the time-varying noise a recent sample of the same noise. For dc or very low-frequency noise this results in a cancellation. This indicates that autozeroing effectively high-pass filters the noise.

In addition to this basic high-pass filtering process, since AZ is a sampling technique, the wideband noise is aliased down to the baseband, increasing the resulting in-band PSD. This is illustrated in Fig. 2 which shows the normalized input-referred noise PSD of the amplifier with and without AZ[1]. Fig. 2(a) shows the effect of the AZ on a 1st-order low-pass filtered white noise having a bandwidth f_c five times larger than the sampling frequency $f_s = 1/T_s$ ($f_c \cdot T_s = 5$) and the different PSD components resulting from the sampling process. It clearly shows that the autozeroed noise PSD is dominated by the foldover component in the Nyquist band due to the aliasing of the broadband white noise. Fig. 2(b) shows the effect of the AZ process on the flicker noise. The baseband $1/f$ noise is zeroed whereas the other bands are also aliased producing an additional foldover term. The AZ amplifier input-referred PSD can be written as

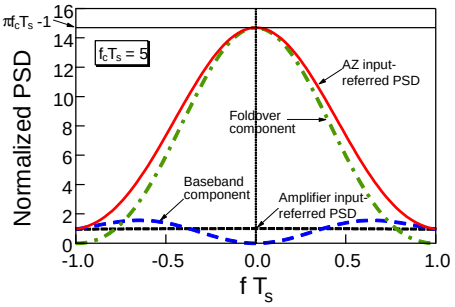

(a) Effect on the broadband white noise where the input-referred noise PSD is normalized to S_0.

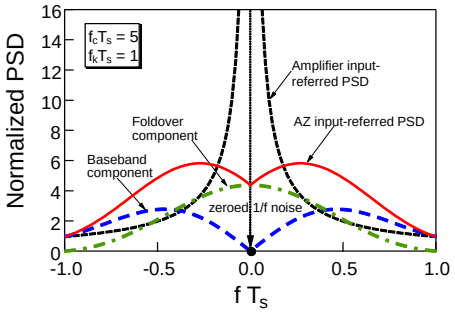

(b) Effect on the flicker noise where the input-referred noise PSD is normalized to $f_k \cdot S_0$.

Fig. 2. Effect of the AZ on the amplifier input-referred PSD.

$$S_{AZ} = |H_0(f)|^2 \cdot S_n(f) + S_{fold}, \tag{2}$$

where $H_0(f) \cong \pi f T_h$ with T_h being the hold time corresponding to the time of the amplification phase, S_n is the original input-referred amplifier noise corresponding to voltage source V_n and S_{fold} is the total foldover component due to aliasing

$$\begin{aligned} S_{fold} \cong S_0 \cdot sinc^2(\pi f T_s)[\pi f_c T_s - 1 \\ + 2 f_k T_s \cdot (ln(2/3 f_c T_s) + 1)]. \end{aligned} \tag{3}$$

The first term in (3) corresponds to the aliased white noise, which usually dominates over the second term corresponding to the aliased flicker noise.

[1]Note that the output PSD are referred to the amplifier input by simply dividing by the DC gain without accounting for the frequency dependence.

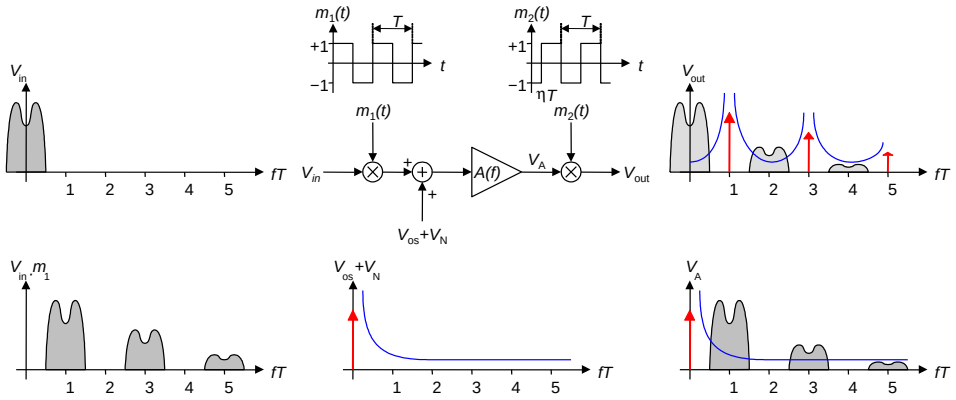

Fig. 3. The chopper stabilization amplification principle.

B. Chopper Stabilization (CS)

Unlike the AZ process, the CS technique does not use sampling, but rather applies modulation to transpose the signal to a higher frequency where there is no $1/f$ noise, and then demodulates it back to the baseband after amplification as illustrated in Fig. 3. Suppose that the input signal has a spectrum limited to half of the chopper frequency so no signal aliasing occurs, and that the amplifier is ideal, with no noise or offset. This input signal is multiplied by the square-wave signal $m_1(t)$ with period T. After this modulation, the signal is transposed to the odd harmonics of the modulation signal. It is then amplified and demodulated back to the original band. Note that the finite amplifier bandwidth may introduce some spurs around the even harmonics of the chopper frequency which have to be low-pass filtered to recover the amplified signal. Note also that in order to maintain a maximum dc gain, the phase shift between the input and the output modulators has to match precisely the phase shift introduced by the amplifier. Since the noise and offset are modulated only once, they are transposed to the odd harmonics of the output chopping square wave, leaving the amplifier ideally without any offset and low-frequency noise. Assuming that the amplifier white noise bandwidth is much larger than the chopper frequency ($f_c T \gg 1$), the total input-referred noise in the baseband is approximately given by

$$S_{CS} \cong S_0 \cdot (1 + 0.8525 f_k T). \tag{4}$$

According to (4), a good trade-off is obtained by choosing the chopper frequency equal to the $1/f$ noise corner frequency ($f_k = 1/T$) for which the resulting white noise PSD increase is then less than 6 dB.

Residual offset is mainly due to clock feedthrough and charge injection of the input modulator. More generally, any spikes caused by the modulator non-idealities and appearing at the amplifier input will be amplified and demodulated by the output modulator, giving rise to a residual dc component. Many techniques have been developed recently to deduce this residual offset.

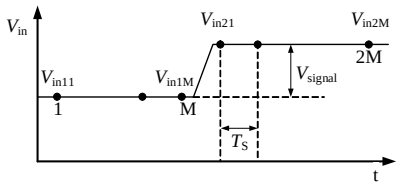

Fig. 4. Timing diagram of the an M-order CMS showing the M samples at the first and second voltage levels.

III. Recent Trends in Noise and Offset Reduction Techniques

An important improvement of the AZ or CDS technique is the use of multiple sampling to average noise prior to the differentiation further reducing $1/f$ noise. This technique has been initially proposed for CMOS image sensors (CIS) [9], [10] and will be discussed in Section III-A.

Most of the recent improvements of the CS noise reduction technique have actually dealt with the reduction of the residual offset and spurs due to glitches introduced by switching. Although the reduction of offset due to glitches remains a difficult problem, it will not be discussed here. The reader is invited to look at the excellent work presented in [11]–[15].

The new noise canceling technique, initially proposed in [16] for RF low noise amplifier, has been reused for a bio-sensor interface where it is combined with CS [17], [18]. It will be presented in Section III-B.

A. Correlated Multiple Sampling (CMS)

Correlated double sampling (CDS) is similar to AZ except that the signal is sampled twice and then the difference is taken between these two samples. It has been introduced initially for image processing in CCD [19], [20]. In a CMOS image sensor (CIS) with pixels based on pinned photodiodes, the sense node is first reset, then the photo-generated charges are transferred to the sense node reducing its voltage. The CDS in the case of CIS is operated by differentiating two samples at the output of the sensor, one after resetting the sense node and the other one after the charge transfer.

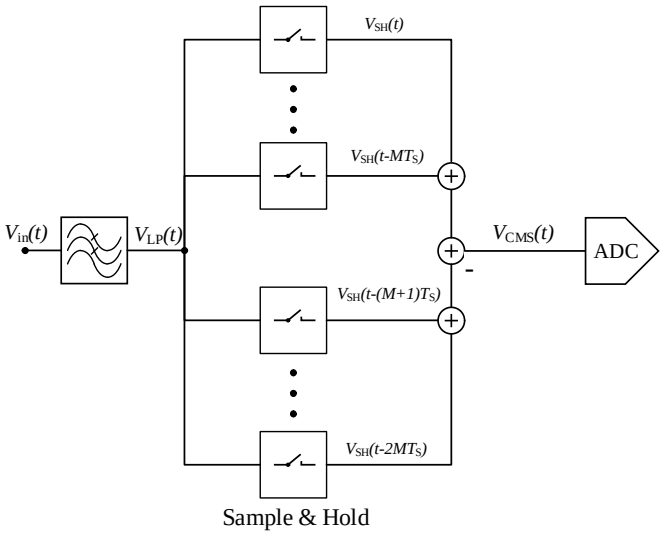

(a) Implementation of the CMS in the analog domain.

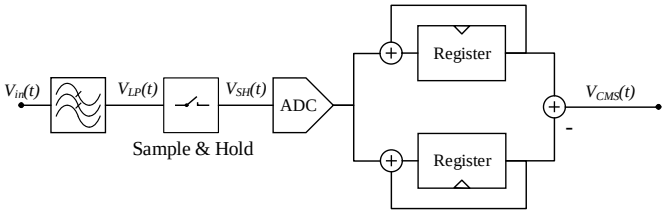

(b) Implementation of the CMS in the digital domain.

Fig. 5. Practical implementations of CMS.

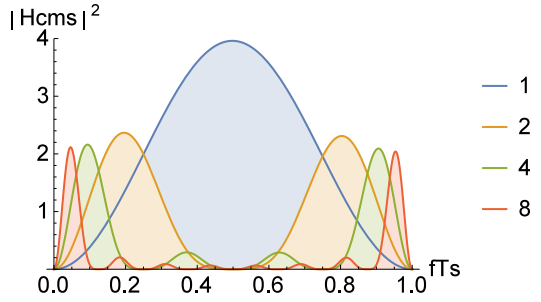

Fig. 6. Plot of the squared absolute value of $|H_{CMS}(f)|^2$

Correlated multiple sampling (CMS) was introduced for CIS in [9], [10]. It combines CDS with averaging. CMS of order M corresponds to averaging M samples at the reset level and M samples after charge transfer and then differentiating the two averages. Fig. 4 shows a typical signal shape on which CMS can be applied. Like auto-zeroing CMS and CDS cancel the offset and reduce low frequency noise.

The main practical implementations of CMS are depicted in Fig. 5. CMS can be performed in the analog domain using sample and holds as shown in Fig. 5(a). This can be implemented using a passive switched capacitors (SC) network or by using an active SC integrator [10]. The CMS can also be performed in the digital domain using registers [21] [22]

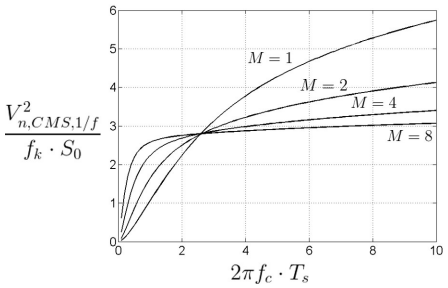

(a) $1/f$ noise

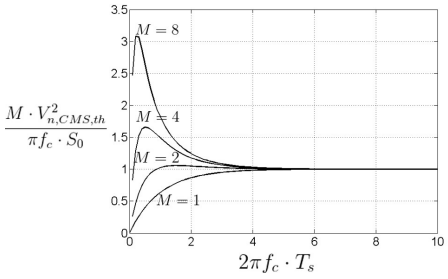

(b) Thermal noise

Fig. 7. Plot of the normalized noise variance at the output of the CMS stage

as shown in Fig. 5(b). Note that both implementations require sample and hold stages with a sampling period of $2MT_S$, where T_S is the duration between samples. T_S is set to give the signal enough time to settle between two consecutive samples. the sample and hold process can be mathematically modeled in time domain by a multiplication by a Dirac trail convoluted with a zero order hold. In time domain, the sampled low-pass-filtered signal can be expressed as

$$V_{SH}(t) = h(t) * \sum_{n=-\infty}^{+\infty} \delta(t - n \cdot 2MT_S) \cdot V_{LP}(t). \qquad (5)$$

where $h(t)$ is the rectangular function that takes unity in $[0, 2MT_S]$ and zero elsewhere. The signal at the output of the CMS can then be expressed in time domain as

$$V_{CMS}(t) = V_{SH}(t) * \frac{1}{M} \sum_{k=0}^{M-1} \delta(t - kT_S) - \delta(t - (k+M)T_S). \qquad (6)$$

In order to investigate the impact of correlated sampling on noise, a noise source with a PSD S_N bandlimited at the first order with a cutoff frequency f_c is considered.

$$S_N(f) = S_0 \left(1 + \frac{f_k}{|f|}\right) \cdot \frac{1}{1 + \left(\frac{f}{f_c}\right)^2}, \qquad (7)$$

The noise PSD at the output of the CMS is obtained by transposing (6) in the Fourier domain

$$S_{N,CMS}(f) = \sum_{n=-\infty}^{+\infty} |H_n(f)|^2 \cdot S_N(f - \frac{n}{2MT_S}), \qquad (8)$$

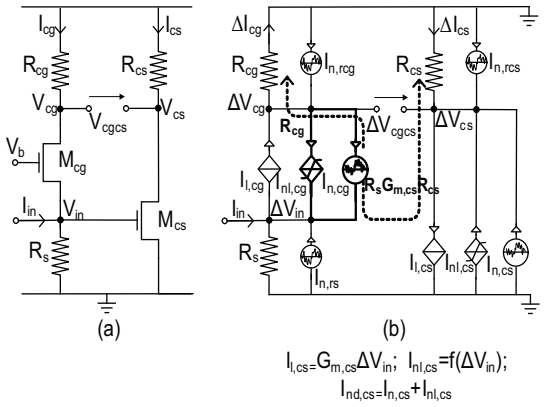

Fig. 8. Principle of the noise canceling TIA.

where

$$|H_n(f)|^2 = sinc^2(\pi f \cdot 2MT_S) \cdot |H_{CMS}(f - \frac{n}{2MT_S})|^2 \quad (9)$$

and

$$|H_{CMS}(f)|^2 = \frac{4}{M^2} \cdot \frac{sin^4(\pi M f T_S)}{sin^2(\pi f T_S)}. \quad (10)$$

The noise variance is obtained by calculating the total noise power. It can be shown that

$$\int_{-\infty}^{+\infty} S_{N,CMS}(f)df = \int_{-\infty}^{+\infty} |H_{CMS}(f)|^2 \cdot S_N(f)df. \quad (11)$$

The term $|H_{CMS}(f)|^2$ representing the impact of correlated sampling on the noise PSD is plotted in Fig. 6 for M ranging between 1 and 8. One can notice that the area delimited by $|H_{CMS}(f)|^2$ is inversely proportional to M, therefore, the withe noise variance at the output of the CMS stage is inversely proportional to M. For all values of M, the CMS transfer function applies a zeroing to the low frequencies, The area delimited by $|H_{CMS}(f)|^2$ reduces by increasing M but the maximum of $|H_{CMS}(f)|^2$ gets closer to the vertical axis. Thus one can assume that $1/f$ noise is also reduced by increasing the CMS order but this reduction reaches a limit for a certain order M. Based on numerical evaluation of the integrated noise PSD expressed in (11), Fig. 7(b) shows the thermal noise variance normalized to $\frac{S_0 \pi f_c}{M}$ and $1/f$ noise variance normalized to $S_0 \cdot f_k$ as a function of $2\pi f_c T_S$. Note that $2\pi f_c T_S$ should be at least equal to 5 for sufficient settling of the signal between two samples. Thermal noise variance before the CMS stage is given by $\frac{S_0 \pi f_c}{2}$, thus, a simple CDS ($M = 1$) doubles the thermal noise variance and a CMS of order M higher than 2 reduces the thermal noise variance by $\frac{M}{2}$. $1/f$ noise is dramatically reduced with a simple CDS due to the zeroing at low frequencies. The $1/f$ noise reduction efficiency increases with the CMS order and reaches a plateau for values of M higher than 8 as shown by Fig. 7(a).

B. Combining Noise Cancelation and Chopper Stabilization

A technique called noise cancelation has been introduced in [16] to reduce the noise in RF circuits such as wideband low-noise amplifiers (LNAs). The basic principle is to take advantage of the fact that the noise in the amplifier is injected at a different node than the signal, resulting in different transfer functions for the noise and for the signal to the output. This enables the noise to be duplicated and canceled at the differential output, whereas the signal is summed. The same principle has recently been used in the front-end of a bio-sensor interface using a common gate (CoGa) transimpedance amplifier (TIA) [17], [18]. In this work, CS could not be used directly at the input because of the required low-impedance which would be difficult to achieve due to the series switches of the input chopper modulator. The $1/f$ noise issue is solved by using the noise canceling principle to reject the main contributor to $1/f$ noise and it is combined with chopping to reject the additional $1/f$ noise coming from the subsequent stages. In this way, the front-end achieves low noise performance without compromising on the input impedance. The canceling principle actually not only cancels $1/f$ noise but also part of the white noise and distortions due to the nonlinearity of the same device, improving the front-end linearity. The principle of the noise canceling TIA is shown in Fig. 8(a). The input current I_{in} is fed at the source of the CoGa stage and the differential output is taken across the output nodes of the CoGa and an additional common-source (CoSo) stages. The main function of the CoSo stage is to cancel the non-idealities (primarily noise and distortion) of the CoGa transistor Mcg by matching the noise transfer function (NTF) along the two paths (CoGa and CoSo paths) in magnitude and phase. The condition for noise cancelation can be derived by equating the noise voltages at the CoGa and CoSo stage outputs, resulting in [17], [18]

$$R_{cg}/R_s = G_{m,cs} \cdot R_{cs}. \quad (12)$$

This condition is valid only within a certain bandwidth. Beyond a certain frequency, the cancelation begins to degrade because of bandwidth limitations due to parasitics. Note that if condition (12) is satisfied, only the noise of M_{cg} gets canceled but not other noise sources like the noise coming from the resistors or from the CoSo transistor. In the noise canceling TIA, while the NTFs are matched along the two paths to achieve noise cancelation, the signal transfer function ($STF = V_{cgcs}/I_{in}$) is matched in magnitude but with opposite phase and this provides amplification of the input current I_{in}. The resulting gain for the noise canceling TIA is simply $R_m = R_{cg}$.

Fig. 9 shows the fully differential implementation of the noise canceling amplifier where the CoGa stage is combined with a chopped differential CoSo stage to eliminate the $1/f$ noise contributed by the CoSo stage. Fig. 10 shows the plot of the measured input-referred noise PSD in the overall front-end with and without noise rejection techniques. As evident from the noise plot, the effect of noise is minimized thanks to the combined effects of canceling and chopping. The input-referred current noise PSD in the overall front-end with canceling and

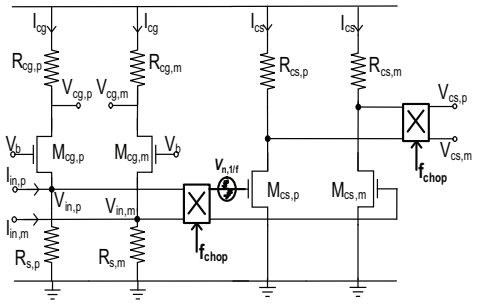

Fig. 9. Schematic of the noise canceling TIA.

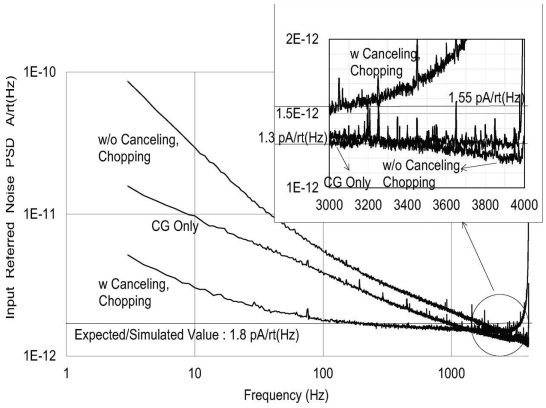

Fig. 10. Measured input-referred noise PSD.

chopping active is measured to be 1.6 $pA/\sqrt{Hz}$ which closely matches with the simulated/expected value of 1.8 $pA/\sqrt{Hz}$. There is still some residual $1/f$ noise due to the limited gain making the following gain stages also contribute.

IV. Conclusion

Noise remains the ultimate limitation for many electronics systems. In low-frequency sensor interfaces, noise is dominated by low-frequency noise ($1/f$ noise) and offset. The latter can be strongly reduced by means of circuit techniques such as AZ and CS. It is recalled that both AZ and CS indeed allow to significantly reduce the $1/f$ noise and offset, but AZ suffers a significant increase in the baseband white noise due to aliasing, whereas CS has no impact on the white noise. New trends in circuit noise reduction techniques are presented. In CMS, noise cancelation is combined with averaging which allows to further reduce $1/f$ noise, but, similarly to AZ, it is also ultimately limited by the aliasing of the broadband white noise. Another technique combining noise cancelation and CS in a TIA for bio-sensors is presented. It allows to maintain a low input impedance required by the TIA, while reducing the noise of the main CoGa stage. CS is then used to cancel the noise of the following stages.

References

[1] C. C. Enz and G. C. Temes, "Circuit Techniques for Reducing the Effects of Op-amp Imperfections: Autozeroing, Correlated Double Sampling, and Chopper Stabilization," *Proceedings of the IEEE*, vol. 84, no. 11, pp. 1584–1614, Nov. 1996.

[2] C. C. Enz, E. A. Vittoz, and F. Krummenacher, "A CMOS Chopper Amplifier," *IEEE J. of Solid-State Circuits*, vol. 22, no. 3, pp. 335–342, June 1987.

[3] B. Razavi, *Principles of Data Conversion System Design*. New York: Wiley-IEEE Press, 1995.

[4] R. Poujois and J. Borel, "A Low Drift Fully Integrated MOSFET Operational Amplifier," *IEEE J. of Solid-State Circuits*, vol. 13, no. 4, pp. 499–503, Aug. 1978.

[5] R. C. Yen and P. R. Gray, "A MOS Switched-capacitor Instrumentation Amplifier," *IEEE J. of Solid-State Circuits*, vol. 17, no. 6, pp. 1008–1013, Dec. 1982.

[6] Y. Chong-Gun and R. L. Geiger, "An Automatic Offset Compensation Scheme with Ping-pong Control for CMOS Operational Amplifiers," *IEEE J. of Solid-State Circuits*, vol. 29, no. 5, pp. 601–610, May 1994.

[7] M. C. W. Coln, "Chopper Stabilization of MOS Operational Amplifiers Using Feed-forward Techniques," *IEEE J. of Solid-State Circuits*, vol. 16, no. 6, pp. 745–748, Dec. 1981.

[8] I. G. Finvers, J. W. Haslett, and F. N. Trofimenkoff, "A High Temperature Precision Amplifier," *IEEE J. of Solid-State Circuits*, vol. 30, pp. 120–128, Feb. 1995.

[9] N. Kawai and S. Kawahito, "Effectiveness of a Correlated Multiple Sampling Differential Averager for Reducing 1/f Noise," *IEICE Electronics Express*, vol. 2, no. 13, pp. 379–383, 2005.

[10] S. Suh, S. Itoh, S. Aoyama, and S. Kawahito, "Column-Parallel Correlated Multiple Sampling Circuits for CMOS Image Sensors and Their Noise Reduction Effects," *Sensors*, vol. 10, no. 10, pp. 9139–9154, Oct. 2010.

[11] J. F. Witte, K. A. A. Makinwa, and J. H. Huijsing, "A CMOS Chopper Offset-Stabilized Opamp," *IEEE J. of Solid-State Circuits*, vol. 42, no. 7, pp. 1529–1535, July 2007.

[12] W. Rong, K. A. A. Makinwa, and J. H. Huijsing, "A Chopper Current-Feedback Instrumentation Amplifier With a 1 mHz $1/f$ Noise Corner and an AC-Coupled Ripple Reduction Loop," *IEEE J. of Solid-State Circuits*, vol. 44, no. 12, pp. 3232–3243, Dec. 2009.

[13] F. Qinwen, F. Sebastiano, J. H. Huijsing, and K. A. A. Makinwa, "A 1.8μW 60 nV/$\sqrt{Hz}$ Capacitively-Coupled Chopper Instrumentation Amplifier in 65 nm CMOS for Wireless Sensor Nodes," *IEEE J. of Solid-State Circuits*, vol. 46, no. 7, pp. 1534–1543, July 2011.

[14] F. Qinwen, J. H. Huijsing, and K. A. A. Makinwa, "A 21 nV/$\sqrt{Hz}$ Chopper-Stabilized Multi-Path Current-Feedback Instrumentation Amplifier With 2μV Offset," *IEEE J. of Solid-State Circuits*, vol. 47, no. 2, pp. 464–475, Feb. 2012.

[15] F. Qinwen, J. Huijsing, and K. A. A. Makinwa, "A Multi-path Chopper-stabilized Capacitively Coupled Operational Amplifier with 20V-input-common-mode Range and 3μV Offset," in *IEEE Int. Solid-State Circuits Conf. Dig. Tech. Papers (ISSCC)*, Feb. 2013, pp. 176–177.

[16] F. Bruccoleri, E. A. M. Klumperink, and B. Nauta, "Wide-band CMOS Low-noise Amplifier Exploiting Thermal Noise Canceling," *IEEE J. of Solid-State Circuits*, vol. 39, no. 2, pp. 275–282, Feb. 2004.

[17] V. Balasubramanian, P. F. Ruedi, and C. Enz, "Noise Canceling Chopper Stabilized Front-end for Electrochemical Biosensors with Improved Dynamic Range," in *IEEE Int.Symp. on Circuits and Systems (ISCAS)*, May 2012, pp. 2215–2218.

[18] V. Balasubramanian, P. F. Ruedi, Y. Temiz, A. Ferretti, C. Guiducci, and C. C. Enz, "A 0.18 μm Biosensor Front-End Based on $1/f$ Noise, Distortion Cancelation and Chopper Stabilization Techniques," *IEEE Trans. on Biomedical Circuits and Systems*, vol. 7, no. 5, pp. 660–673, Oct. 2013.

[19] M. H. White, D. R. Lampe, F. C. Blaha, and I. A. Mack, "Characterization of Surface Channel CCD Image Arrays at Low Light Levels," *IEEE J. of Solid-State Circuits*, vol. 9, no. 1, pp. 1–12, Feb. 1974.

[20] R. J. Kansy, "Response of a Correlated Double Sampling Circuit to 1/f Noise," *IEEE J. of Solid-State Circuits*, vol. 15, no. 3, pp. 373–375, June 1980.

[21] Y. Lim, K. Koh, K. Kim, H. Yang, J. Kim, Y. Jeong, S. Lee, H. Lee, S.-H. Lim, Y. Han, J. Kim, J. Yun, S. Ham, and Y.-T. Lee, "A 1.1e- temporal noise 1/3.2-inch 8mpixel cmos image sensor using pseudo-multiple sampling," in *Solid-State Circuits Conference Digest of Technical Papers (ISSCC), 2010 IEEE International*, 2010, pp. 396–397.

[22] Y. Chen, Y. Xu, Y. Chae, A. Mierop, X. Wang, and A. Theuwissen, "A 0.7e rms-temporal-readout-noise cmos image sensor for low-light-level imaging," in *Solid-State Circuits Conference Digest of Technical Papers (ISSCC), 2012 IEEE International*, 2012, pp. 384–386.